Addition of organic acids to acid mine drainage polluted wetland sediment leads to microbial community structure and functional changes and improved water quality

Oscar E. Aguinaga [a, b], Keith N. White [a], Andrew P. Dean [c], and Jon K. Pittman [a, *]

[a] Department of Earth and Environmental Sciences, School of Natural Sciences, Faculty of Science and Engineering, The University of Manchester, Michael Smith Building, Oxford Road, Manchester M13 9PT, UK

[b] Departamento de Ingeniería, Facultad de Ciencias y Filosofía, Universidad Peruana Cayetano Heredia, Lima, Peru

[c] Department of Natural Sciences, Faculty of Science and Engineering, Manchester Metropolitan University, Oxford Road, Manchester M1 5GD, UK

* Corresponding author.

E-mail address: jon.pittman@manchester.ac.uk (J. K. Pittman).

Department of Earth and Environmental Sciences, School of Natural Sciences, Faculty of Science and Engineering, The University of Manchester, Michael Smith Building, Oxford Road, Manchester M13 9PT, UK. Tel: +44 161 275 5235.

Abstract

Acid mine drainage (AMD) is a serious environmental problem worldwide that requires efficient and sustainable remediation technologies including the use of biological mechanisms. A key challenge for AMD bioremediation is to provide optimal conditions for microbial-mediated immobilisation of trace metals. Although organic carbon and oxygen can enhance treatment efficiency, the effect on microbial communities is unclear. In this study, surface sediments from a natural wetland with proven efficiency for AMD bioremediation were artificially exposed to oxygen (by aeration) and/or organic carbon (in the form of mixed organic acids) and incubated under laboratory conditions. In addition to measuring changes in water chemistry, a metagenomics approach was used to determine changes in sediment bacterial, archaeal and fungal community structure, and functional gene abundance. The addition of organic carbon produced major changes in the abundance of microorganisms related to iron and sulfur metabolism (including *Geobacter* and *Pelobacter*) and increased levels of particulate metals via sulfate reduction. Aeration resulted in an increase in *Sideroxidans* abundance but no significant changes in metal chemistry were observed. The study concludes that the utilisation of organic carbon by microorganisms is more important for achieving efficient AMD treatment than the availability of oxygen, yet the combination of oxygen with organic carbon addition did not inhibit the improvements to water quality.

Keywords: Acid mine drainage; Bacterial community; Fungal community; Metagenomics; Metal pollution; Microbial bioremediation

1. Introduction

Metal and coal mining from abandoned and active mines releases significant amounts of trace metals that are harmful to ecosystem function and human health (Azapagic, 2004). These mine effluents are often highly acidic due to the oxidation of metal sulfide minerals yielding a metal-rich acid mine drainage (AMD). This is generated by exposure of pyrite minerals to air and water, with microbial activity further enhancing these reactions (Chen et al., 2016). Although AMD is very damaging to most biota, AMD impacted environments provide an important ecological niche for microorganisms that have adapted to these extreme conditions. These adapted organisms have enhanced metabolic capabilities for the cycling and modification of iron (Fe), sulfur (S), carbon and other trace metals, and the removal of acidity (Méndez-García et al., 2015; Huang et al., 2016). These microbial processes may be utilised for 'passive' AMD remediation methods that require minimal maintenance and rely on the use of natural processes (Johnson and Hallberg, 2005), such as within constructed wetlands and in bioreactor systems, where Fe oxidation drives formation of insoluble Fe precipitates such as ferrihydride, and sulfate reduction produces hydrogen sulfide (Neculita et al., 2007; Clyde et al., 2016). This in turn increases pH and generates particulate metal sulfides to reduce the dissolved metal concentration in the water column (Hedrich and Johnson, 2014; Aguinaga et al., 2019). In both natural and constructed wetlands this remediation is achieved in part through the interaction of plants with rhizosphere sediment bacterial, archaeal and fungal communities. The wetlands maintain a diverse microbial community that mediates various biogeochemical activities to allow AMD remediation (Aguinaga et al., 2018). The plants also provide organic carbon and oxygen to the rhizosphere sediment, as well as reducing the flow rate of the drainage stream and providing anchorage for the sediment (August et al., 2002; Dean et al., 2013).

It has previously been proposed that the efficiency of passive mine drainage remediation using constructed wetlands and bioreactors can be enhanced by simple interventions (giving a 'semi-passive' approach) including addition of organic carbon substrates, to sustain heterotrophic sulfate-reducing bacteria (SRB) (Gibert et al., 2004;

71 Costa and Duarte, 2005; Jimenez-Castaneda et al., 2020), or manipulation of oxygen levels,
72 such as by aeration to enhance Fe oxidation (Kirby et al., 2009; Chen and Jiang, 2012;
73 Fernandez-Rojo et al., 2017). For example, altering the type and amount of organic carbon
74 substrates will select for, and enhance the growth of microorganisms carrying out these
75 remediation processes (Hiibel et al., 2011; Zhang and Wang, 2014), especially since the
76 availability of dissolved organic carbon sources is often a major limiting factor (Neculita et
77 al., 2007). However, the presence of oxygen will enhance degradation of organic matter and
78 will suppress SRB activities (Marschall et al., 1993), thus it would seem counter-productive
79 to allow a carbon-utilising AMD bioremediation system to become aerobic. Nevertheless, it is
80 clear that microorganisms that are generally considered to be anaerobic, such as SRB, can
81 tolerate some oxygen exposure (Canfield and Des Marais, 1991; Kjeldsen et al., 2004).
82 Moreover, wetland environments that can perform AMD remediation are typically rich in
83 organic matter but have significant sub-surface aerobic zones, caused by water flow and
84 oxygenation by the wetland vegetation (Dean et al., 2013).
85 A direct comparison and combination of aeration and organic carbon addition has
86 rarely been performed in a controlled manner, in order to understand exactly what impacts
87 organic acid addition combined with oxygenation has on the wider prokaryotic and fungal
88 communities within an AMD environment, and how this affects water chemistry. While many
89 previous studies have examined bacterial and archaeal community structure and function
90 within various AMD environments (Huang et al., 2016), less is known about community
91 structure and function within AMD contaminated wetlands, particularly in the aerobic surface
92 sediment-water interface (Aguinaga et al., 2018). The composition and role of fungal
93 communities within AMD environments are also poorly understood (Das et al., 2009; Mosier
94 et al., 2016).
95 We previously examined how bacterial communities within sediments from a natural
96 wetland respond to AMD from analysis of field samples (Aguinaga et al., 2018). This wetland
97 is exposed to highly acidic (pH 2 – 3) AMD, rich in metals including Fe, copper (Cu) and zinc
98 (Zn) (Dean et al., 2013). The aim of this present study was to use metagenomics

approaches to generate new insights into the bacterial, archaeal, and fungal taxonomy and metabolism in AMD-adapted, surface sediments taken from the same wetland examined previously, but artificially exposed to oxygen by aeration and/or low molecular weight organic acids during a 3-month incubation period. The objectives were (1) to quantify changes in the sediment microbial community in response to oxygen and/or organic carbon addition, and (2) to quantify water chemistry characteristics and changes in predicted functional (metabolic) activities, in order to connect microbial metabolism to remediation of AMD. We hypothesise that the addition of oxygen would increase metal oxidation reactions and select for aerobic microorganisms, while that the addition of organic acids would select for heterotrophic microorganisms, such as SRB, that would enhance AMD remediation. We further hypothesise that combined oxygen and organic carbon addition would alter the microbial community structure, yet may reduce the abundance of some anaerobic microorganisms, but would still improve water chemistry characteristics with respect to reducing dissolved metal concentrations.

2. Materials and methods

2.1. Sediment preparation

Sediment samples containing natural microbial communities were obtained from the middle of a wetland in Anglesey, UK, through which a small river (southern Afon Goch) flows, and which receives AMD pollution from an abandoned Cu mine at Parys Mountain (Dean et al., 2013; Aguinaga et al., 2018). These surface sediments are rich in trace metals (0.2 – 10 mg g^{-1} Al, 0.2 – 0.6 mg g^{-1} As, 1 – 5 mg g^{-1} Cu, 90 – 140 mg g^{-1} Fe, 0.1 – 2 mg g^{-1} Pb, 0.5 – 3 mg g^{-1} Zn), and sulfur (3 – 8 mg g^{-1} S), and with dissolved organic carbon (DOC) and nitrogen concentrations of approximately 0.5 mg g^{-1} and 0.01 mg g^{-1}, respectively (Aguinaga et al., 2019). They are composed of light brown, medium-to-fine sediment and contain larger soil particles and plant debris. The location of the sample site was Lat. 53°22'54.7" N, Long. 4°19'42.4" W. Sediments surrounding *Juncus* sp. roots within a stand

were collected to approximately 1 cm depth using a plastic scoop and sealed in a plastic bag. On return to the laboratory, the sediment sample (approximately 5 kg in total) was mixed together and refrigerated at 4 °C until use. To assess the extent to which chemical changes were microbial rather than abiotic, half of the sediment sample (2.5 kg) was sterilised by irradiation. This sample was split into 250 g aliquots in polyethylene bags, and gamma-irradiated at a dose of 40 kGy using a ^{60}Co gamma irradiation source (Dalton Cumbrian Facility, University of Manchester, UK). Previous irradiation dose analysis with different soil types demonstrated that most bacterial groups were eliminated at doses between 20 – 25 kGy and fungi were eliminated between 5 – 10 kGy (reviewed by McNamara et al., 2003), thus the 40 kGy dose used here was likely to eliminate virtually all microorganisms naturally present within the sediment at the start of the microcosm incubation.

2.2. Microcosm preparation

Microcosms contained natural wetland sediment and artificial AMD water, and consisted of an untreated group (UNT), and three treatment groups of either addition of oxygen by aeration (OXY), addition of low molecular weight organic acids (LOA), or both aeration and organic acids (LOX). There were five replicates per treatment group. Microcosms each consisting of 5 g of non-irradiated or irradiated sediments were prepared in 50 mL open-topped polypropylene tubes. A total of 20 mL of a simplified artificial AMD solution (10 mg L^{-1} Fe, 5 mg L^{-1} Zn and 2 mg L^{-1} Cu, as $FeSO_4 \cdot 7H_2O$, $ZnSO_4 \cdot 7H_2O$, and $CuSO_4 \cdot 5H_2O$, respectively, and pH 3.0 – 3.5 using H_2SO_4) was added to each tube. The concentrations of the trace metals and the pH value were equivalent to the AMD at the wetland site (Dean et al., 2013; Aguinaga et al., 2018), while the use of an artificial AMD solution allowed examination of a specified number of chemical variables. For the OXY and LOX microcosms, filtered air was continuously introduced into the water column using an air pump. This gave a dissolved oxygen (DO) concentration of approximately 2.15 mg L^{-1} (20% saturation), which was equivalent to DO concentrations seen in many constructed wetlands

(Liu et al., 2016). For the LOA and LOX microcosms, a mixture of low molecular weight organic acids (Supelco, CRM46975) containing acetic acid, formic acid, propionic acid, isobutyric acid, butyric acid, isovaleric acid, valeric acid, isocaproic acid, hexanoic acid and n-heptanoic acid was added into the water every 10 days at a final concentration of 10 mg L^{-1}, which was equivalent to DOC concentrations seen in previous pilot-scale constructed wetlands (Huang et al., 2005). The UNT microcosms had no aeration or organic acid addition. The 40 non-irradiated and irradiated sediment microcosms were incubated over 88 days at a constant temperature of 10 °C. Previous sediment incubation experiments had detected changes in microbial-mediated Fe^{2+} oxidation after 55 days incubation (Senko et al., 2011) and influence of addition of carbon sources on bacterial diversity and activity has been previously investigated over 60 days (Adams et al., 2007), therefore an 88 day incubation was deemed to be an appropriate time period to also observe microbial community changes in response to the treatments. The water level of the AMD solution was maintained by addition of distilled water when volume was lost due to evaporation and samples taken for water chemistry measurements (Section 2.3). Fe, Zn, Cu, S, DO, DOC concentrations and water chemistry at the start of the incubation period (measured at Day-1) are shown in Figure S1 and Table S1.

2.3. Measurement and analysis of water chemistry variables and sediment metals

Artificial AMD pH values in each microcosm were monitored using a portable pH meter (HANNA Instruments, UK) and maintained (pH 3.0 – 3.5) using H_2SO_4 when needed. DO in the water was measured using an optical oxygen probe (Pyro Science, Germany). Total and inorganic C concentrations were obtained using a Shimadzu 5000 A TOC analyser (Shimadzu Limited, UK), as described previously (Aguinaga et al., 2019). DOC in the water was measured by subtracting inorganic C values from total C.

Water samples for metal measurement were taken and filtered through a 0.45 µm cellulose acetate filter. Filtered samples were acidified to 2% (v/v) with ultra-pure nitric acid while the filters were retained for determination of metal particulates. Sediment samples

were collected at the end of the incubation period. Filters containing suspended particulates and the sediment samples were dried at 80 °C for 48 h. The dried sediments were passed through a 250 µm mesh stainless steel sieve to homogenize particles prior to digestion. The filter papers and 100 mg of sediments were digested in 67% (v/v) ultra-pure nitric acid for 4 h at 70 °C. Digests were then diluted to 2% (v/v) nitric acid in deionized Milli-Q water (Millipore, UK). Water samples and digests were analysed by inductively coupled plasma atomic emission spectroscopy (ICP-AES) using a Perkin-Elmer Optima 5300 for Al, As, Cd, Cu, Fe, Mn, Pb, S and Zn. Calibration was performed using an internal standard, which was a matrix matched serial dilution of Specpure multi element plasma standard solution 4 (Alfa Aesar, USA).

Fe^{2+}, sulfate and sulfide concentrations in the water samples were determined using 1,10-Phenanthroline, Methylene Blue and SulfaVer 4 based measurements, respectively, using a DR900 Multiparameter Portable Colorimeter (Hach, USA). Fe^{3+} concentrations were determined as the difference between Fe^{2+} and total Fe concentrations.

Statistical comparison of water and sediment chemistry data was performed using one–way ANOVA ($p < 0.05$) and Tukey's multiple comparison post hoc test using GraphPad Prism (v.5). Principal component analysis (PCA) of water chemistry data (dissolved and particulate, and sulfur and iron species) was performed using R vegan package v.2.5-6. Values were normalised prior to PCA.

2.4. DNA extraction and shotgun metagenome sequencing

At the end of the incubation period, total DNA was extracted from 0.5 g of sediments from each non-irradiated microcosm using a PowerSoil DNA Extraction kit (Qiagen, Germany) according to the manufacturer's instructions. DNA was not extracted from the irradiated sediments. DNA libraries were prepared using a NEBNext Ultra DNA Library Prep Kit for Illumina and a NEBNext Multiplex Oligos for Illumina kit (New England Biolabs, USA), both according to the manufacturer's instructions. Paired–end sequencing of the whole metagenome of each library was performed using an Illumina HiSeq3000 with 2 x 150 bp

read length (Leeds Institute of Molecular Medicine Next Generation Sequencing Facility, UK). Approximately 13 – 14 million sequence reads were generated from each library (Table S2). Raw sequence data (FASTQ files) were deposited in the European Nucleotide Archive (Project accession number: PRJEB43376).

2.5. Sequence data analysis

Forward and reverse reads from each microcosm sample were paired using the PEAR (version 0.9.8) merger (Zhang et al., 2014). Paired sequences were then trimmed using Trimmomatic (version 0.38) (Bolger et al., 2014) for removing low-quality reads. FASTQ files from trimmed sequences were uploaded to the MG-RAST server (Meyer et al., 2008) for processing and annotation. Taxonomic assignment of 16S and 18S rRNA gene sequence reads was performed using the Reference Sequence (RefSeq) collection (release 89) (Pruitt et al., 2007) and by applying standard MG-RAST specifications (maximum e-value of 1e−5, a minimum identity of 97%, and a minimum alignment length cut-off of 15). The taxonomic data generated from each sample are shown in Table S2 and Data Sheet S1. In order to evaluate the microbial alpha diversity in each sample, Shannon–Wiener diversity index, Pielou's evenness index, Chao1 species richness estimator and Berger–Parker dominance index were calculated from the genus level datasets using the software PAST (version 4.03) (Hammer et al., 2001). Using the R vegan package v.2.5-6, the taxonomic dataset was analysed by similarity percentage (SIMPER) analysis (Clarke, 1993) to identify taxa discriminating between treatments and their contribution. Functional classification of the metagenomic data was performed through the annotation pipeline from MG-RAST using the SEED subsystem database (Overbeek et al., 2014). The functional data was classified using a maximum e-value of 1e−5, a minimum identity of 60%, and a minimum alignment length of 15 amino acids for proteins (default settings). The predicted functional gene data generated from each sample are shown in Table S2 and Data Sheet S2. Taxonomic and functional data specific for prokaryotes (archaea and bacteria) and fungi were analysed by non–metric multidimensional scaling (NMDS) and water chemistry vectors were fitted onto the

ordinations to link chemistry data with sequence similarity assemblages using the ENVFIT function in the vegan package. Heat maps of genes were generated using Morpheus software (software.broadinstitute.org/Morpheus).

3. Results

3.1. Microbial induction of metal precipitation

At the start of the incubation period (Day-1) there were no water chemistry differences between any of the microcosm treatment groups (Fig. S1). After the 88-day incubation period, examination of water chemistry parameters demonstrated a clear differentiation between the organic acid amended microcosms (LOA and LOX) in comparison to the aerated alone (OXY) and untreated (UNT) microcosms (Fig. 1). However, there was much less distinction between OXY and UNT microcosms, and no distinction between LOA and LOX, as determined by PCA, due to identical water chemistry measurements within these microcosms for all parameters except for particulate Zn (Fig. 1A). The clustering of LOA and LOX treatments from OXY and UNT on the basis of PC1 was determined by the presence of particulate trace metals and oxidation of Fe and S (Fe^{3+} and sulfide) correlating with the LOA and LOX microcosms, while there was a significant correlation between dissolved trace metals and reduction of Fe and S (Fe^{2+} and sulfate). In particular, concentration of sulfide and particulate S was significantly higher in the water column of the LOA and LOX microcosms by the end of the incubation period, and particulate Fe concentration, and particulate Cu concentration increased in the LOA and LOX treatments, while dissolved Zn concentrations were significantly reduced (Fig. 1B). Furthermore, Fe^{3+} and particulate Zn concentration was increased in the LOX treatment compared to the UNT microcosm. Notably, the concentration of particulate S was significantly lower in the OXY microcosms at the end of the incubation period compared to the LOA and LOX treatments (Fig. 1B).

Comparison between the non-irradiated sediment microcosms and the irradiated sediment microcosms at the end of the incubation indicate that most of the observed water chemistry changes were due to biological processes derived from the native microbiota, since these would have been essentially eliminated by the irradiation process. For example, the low concentration of sulfate and dissolved S in all microcosms at the end of the incubation period was not seen in the irradiated microcosms, while the relative increase in sulfide and particulate S in the LOA and LOX treatments was also abolished by irradiation (Fig. 1B). Furthermore, the high concentration of particulate trace metals, such as particulate Cu, at the end of the incubation period was wholly absent in the irradiated microcosms. While some abiotic processes have occurred; for example, oxidation of Fe was observed in both the irradiated and non-irradiated microcosms (Fig. 1B), together these results indicate the presence of microbiological processes driving changes to S, Fe and trace metal chemistry in the water column.

Due to the very high background concentrations of metals and S in the natural sediments, no significant changes in element concentrations were observed in the sediments after incubation, whether or not the sediments had been irradiated (Fig. S2). During incubation, DO in the water column was maintained at approximately 20% saturation in the aerated treatments (OXY and LOX) in contrast to the significantly lower DO (2 – 3% saturation) in the non-aerated treatments (UNT and LOA) (Table S1). Addition of organic acids in the LOA and LOX microcosms gave rise to significantly higher DOC concentrations. These were replenished at regular intervals during the incubation period but by the end of incubation DOC concentration was slightly reduced in these microcosms (Table S1), which was indicative of carbon utilisation by microorganisms.

3.2. Prokaryote and fungal community structure

Alpha diversity metrics derived from genus level data showed an increase in the number of individual prokaryotes (Fig. 2A) in the OXY and LOX treatments when compared with the control (UNT). While there was no difference in Chao-1 derived species richness

between treatments, Shannon-Wiener diversity and Evenness values were significantly reduced in the OXY treatments compared to UNT, and these values were further significantly reduced in the LOA and LOX treatments (Fig. 2A). In contrast, the LOA and LOX treatments with organic acid addition showed a marked increase in Berger-Parker dominance index values compared to the OXY and UNT groups. This increased dominance of certain taxa in the LOA and LOX treatments is seen in a family level taxonomic bar plot, showing a marked dominance in relative abundance of Geobacteraceae and an increase in Pelobacteraceae in these microcosms compared to the UNT and OXY treatments (Fig. 3A). In contrast, there were slight decreases in abundance of other taxa in the LOA and LOX microcosms including a reduction in Burkholderiaceae, Comamonadaceae, and Gallionellaceae, while Acidobacteraceae and Solibacteraceae were reduced specifically in the LOX treatment compared to that in the other treatments. Rhodocyclaceae showed increased abundance in both aerated treatments (OXY and LOX), but particularly in the OXY microcosms (Fig. 3A). An examination of archaea alpha diversity data (Fig. S3A; Table S3) showed very few differences between OXY, LOA and LOX treatments, but there were significant reductions between these microcosms and the UNT microcosms on the basis of Shannon-Wiener diversity and evenness. In contrast, the data for bacterial taxa alone (Fig. S3B; Table S4) had an identical profile to the full prokaryote alpha diversity data.

Fungal alpha diversity data (Fig. 2B; Table S5) indicated very few changes between treatments except that the LOX microcosms had the lowest number of individuals and the OXY treatment gave the lowest Shannon-Wiener diversity index value. There was no significant difference for other diversity metrics between treatments. Likewise, there were no obvious differences in relative abundance of fungal taxa between microcosms at the family level with respect to treatment (Fig. 3B).

Since there was substantial prokaryote community variation seen between treatments, SIMPER analysis was performed to identify individual taxa at the genus level that explained the variation within the microcosm community structures. There are 26 taxa (all bacteria) that explain the majority of the community assemblage of prokaryotes between

322 the four treatments, with *Geobacter* and *Pelobacter* as key contributors of this assemblage,
323 and main contributors of dissimilarity between treatments (Fig. 4). SIMPER performed pair-
324 wise comparisons between each treatment (Table S6) and showed that *Geobacter* was the
325 main contributor in explaining the dissimilarity between the UNT and LOA, UNT and LOX,
326 OXY and LOA, and OXY and LOX treatments. Other taxa that were important in determining
327 variation between treatments included *Sideroxydans* and *Burkholderia*, which were most
328 abundant in the OXY microcosms; and *Dechloromonas*, which was an important determinant
329 for variation between the aerated and non-aerated treatments, and showed the highest
330 abundance in the OXY and LOX microcosms (Fig. 4).
331 The microbial community structure variation between treatments was further
332 demonstrated by NMDS analysis (Fig. 5). Clustering of microcosm samples on the basis of
333 prokaryotic taxonomy allowed clear differentiation of all four treatments but also showed
334 separation of the LOA and LOX samples from the UNT and OXY samples (Fig. 5A).
335 Incorporating water chemistry variables into the NMDS showed an identical correlation
336 between these chemical variables and the microcosms as seen by PCA (Fig. 1A). For
337 example, there was a strong significant correlation between the particulate metals and S,
338 sulfide and Fe^{3+}, and the LOA and LOX samples (Fig. 5A). Although the analysis of the
339 fungal community data by alpha diversity and taxa abundance showed little variation
340 between treatments, NMDS clustering of the microcosms on the basis of fungal taxonomy
341 did show separation between samples for all four treatments (Fig. 5B). In particular, there
342 was stronger separation between the OXY samples and other treatments. However, LOA
343 replicates showed poor clustering. Dissolved S and Cu showed a significant correlation with
344 the OXY treatments and a negative correlation with Fe^{3+}, dissolved Fe, particulate S and
345 sulfide (Fig. 5B).
346
347 *3.3. Consequence of microbial community structure variation on functional gene availability*
348 Almost 7000 different classes of genes with predicted function were identified from
349 the metagenome sequence read libraries generated from each microcosm sample. These

functional genes were classified at the three SEED classification levels and differentiated between prokaryotes and fungal genome data (Data Sheet S2). There were 2.1 – 3.6 million functional genes in total identified from each sample (Table S2), although the majority of these were from bacteria and archaea with only a very small number of fungal genes predicted (approximately 1000 – 1500 genes per sample). There were less total prokaryotic functional genes from the UNT samples (1.8 – 2.4 million) compared to the other three treatments (2.2 – 3.6 million).

NMDS analysis was repeated on the basis of these functional genes. The prokaryotic data showed a very similar clustering of the microcosm samples on the basis of functional genes (Fig. 5C) as seen on the basis of taxonomy (Fig. 5A), although the correlation pattern with water chemistry variables was slightly different, such that there was a stronger significant correlation between particulate trace metals (except for Zn), sulfide and Fe^{3+} with the OXY samples. NMDS analysis based on fungal functional gene data was also performed (Fig. 5D). OXY treatments showed no defined clustering compared to the other treatments, but the UNT, LOA and LOX treatments were clearly defined.

Hierarchical clustering of all functional genes in a heat map showed that the relative abundance of the prokaryotic genes strongly cluster on the basis of the four treatments (Fig. S4), whereas there was much weaker clustering of the functional genes from fungi on the basis of treatment (Fig. S5). Likewise, there was much stronger patterns of variation in relative gene abundance between treatments within the prokaryotic dataset (Fig. S6) than between the fungal dataset (Fig. S7). Level 1 classification of the genes group them into 28 classes (Data Sheet S2), of which ten classes that are relevant to bacterial metabolism, metal chemistry and stress response were examined in more detail (Fig. 6). OXY treatments showed significantly higher relative abundance in genes related to lipid metabolism, S metabolism, nitrogen metabolism and stress response, and lower relative abundance in genes related to phosphorus metabolism compared to UNT and other treatments. In particular, genes encoding activities for sulfur oxidation and sulfite reduction (Fig. S8), nitrate and nitrite sensing, reduction and transport (Fig. S9) and oxidative stress response,

including stress-inducible transcriptional regulators and chaperones (Fig. S10) had higher relative presence in the OXY microcosm sediments. LOA and LOX treatments showed significantly higher relative abundance in genes related to respiration, and Fe acquisition and metabolism compared to UNT and OXY (Fig. 6). In particular, genes related to Fe binding and transport showed higher relative abundance in the LOA and LOX microcosms (Fig. S11). In the LOA and LOX treatments there was increased presence of a large number of genes related to aerobic cellular respiration, in particular components of oxidative phosphorylation (Fig. S12). For all treatments there was a mixed picture of reduced and increased abundance of various central carbohydrate metabolism genes (Fig. S13), while there was mostly reduced abundance of genes for carbohydrate degradation in the LOA and LOX treatments compared to OXY (Fig. S14). Relative abundance of genes related to protein metabolism and phosphorus metabolism were higher in the UNT samples compared to the others (Fig. 6). The fungal data indicated functional gene differences between the UNT samples and other treatments including for carbohydrate genes, membrane transport, and protein metabolism (Fig. S7). In contrast, the LOA treatment showed higher relative abundance of S metabolism genes.

4. Discussion

In this study, significant changes to the water chemistry and microbial community structure of AMD impacted wetland sediment microcosms were observed following the addition of organic carbon (with or without aeration), with less substantial changes observed following artificial aeration alone. Changes in metal and S chemistry within the water column can be due to both abiotic and biotic mechanisms. The data from irradiated sediments, which would have lost the vast majority of original microbiota (McNamara et al., 2003), showed only minor changes in water chemistry, indicating that the water chemistry changes observed in the non-irradiated sediment microcosms following addition of organic acids or aeration were primarily a result of microbial activity rather than abiotic processes. The most substantial of these changes were increased concentration of particulate Fe, Cu and S.

These would have been mainly due to the formation of metal sulfide precipitates due to sulfate reduction and the accumulation of sulfides, which were observed in the non-irradiated LOA and LOX microcosms, but not in the respective irradiated microcosms. These findings are in line with previous experiments in natural and artificial environments showing that biological mechanisms are the dominant processes in mediating metal chemistry changes, notably Fe oxidation by Fe oxidising bacteria (de Vet et al., 2011), and the formation of sulfides by SRB (Meier et al., 2012; van der Graaf et al., 2020).

Various environmental factors are important in the efficiency of these microbial-mediated activities, such as oxygen, pH and redox potential. Sulfate reduction metabolism can be inhibited by the presence of oxygen and many SRB are considered to be strictly anaerobic (Marschall et al., 1993). Yet environments such as wetlands that are both rich in organic matter and contain sub-surface aerobic zones, typically mediate AMD remediation in part by promoting sulfate reduction activities (Webb et al., 1998; August et al., 2002; Dean et al., 2013), and this was one of the reasons why this study aimed to examine the combined consequence of organic acid addition and aeration. There was no significant difference in concentration of sulfides and particulate S between the LOA and LOX microcosms, indicating that sulfate reduction activities were equivalent between both treatments and potentially occurring in an oxygen-rich environment, which has been seen previously (Canfield and Des Marais, 1991). The addition of aeration may also enhance broad carbon substrate utilisation (Salomo et al., 2009). Low pH can also inhibit microbial sulfate reduction, although SRB activities at pH 3 – 3.5 (the pH conditions maintained here) have been previously observed (Elliott et al., 1998). Redox potential measurements were not performed during this study but this is also an important parameter of metal speciation and for microbial activities (Johnson et al., 2012; Karimian et al., 2018). For example, SRB activities are often enhanced under redox potential values of typically -100 mV to -200 mV in anoxic sediment (Gibert et al., 2004), while addition of organic matter can modify reductive conditions in wetland soils, which stimulates pH increase by SRB metabolism (Jayalath et

al., 2016). However, in the sub-surface and water column where Fe oxidation occurs, the redox conditions will be very different (electropositive).

Although changes were seen in structures of bacterial, archaeal and fungal communities, the archaeal and fungal presence and observed changes were much lower than for the bacteria (51 – 62 fungal taxa and approximately 11,600 total fungal OTUs per microcosm and 60 – 61 archaeal taxa and approximately 200,000 total archaeal OTUs per microcosm versus 583 – 594 bacterial taxa and approximately 7 million total bacterial OTUs per microcosm). The presence and role of archaea in AMD environments have been well studied, and as seen here, they usually make up a small proportion of AMD communities and have been linked with various Fe and S oxidation activities, as well as methanogenesis (Chen et al., 2016; Wang et al., 2018). Fungi are less abundant in response to flooding and in wetland environments generally (Moche et al., 2015). However, in many AMD environments fungi play an important role in carbon and nitrogen cycling (Mosier et al., 2016), and tolerance to metal toxicity (Seena et al., 2020). The fungal community did not significantly change with treatment, including after the addition of carbon, which gave rise to the most substantial bacterial community shifts. The stability of fungal communities has been previously described in other AMD impacted environments (Wang et al., 2018; Ye et al., 2020).

All three treatments (OXY, LOA, LOX) resulted in changes to the prokaryotic communities in comparison to the UNT microcosms. Oxygen addition, via aeration into the water overlying the sediments would potentially increase the aerobic bacterial activity, and reduce anaerobic activity. However, the DO concentration (~20% O_2 saturation) was still fairly low in the OXY and LOX microcosms, indicative of microbial activity breaking down organic matter, and it is likely that anaerobic microenvironments will have remained within the sediments, even with increased oxygen supply. In contrast, the non-aerated microcosms (UNT and LOA) were almost anoxic (<3% O_2 saturation), and suitable for anaerobic bacterial activities. Thus, while the addition of oxygen would have altered the balance of anaerobic/aerobic activity, little change was observed in the water chemistry and bacteria

community. It is possible that the timescale of this experiment was not long enough to see substantial aeration-induced community changes, in contrast to the organic acid-induced changes that were observed. However, one notable change was the increased abundance of *Sideroxydans* in the OXY treatment. *Sideroxydans* is a microaerophilic chemolithoautotroph, and couples the oxidation of Fe to the reduction of oxygen (Beckwith et al., 2015), while fixing CO_2. The addition of air in this treatment may have increased the availability of microaerobic niches, as well as the availability of CO_2, favouring these particular bacteria, which were likely out-competed by heterotrophic bacteria when organic acids were added to the microcosms in the LOX treatment.

The data in this study showed that carbon addition via organic acids was more important than aeration alone in driving biologically mediated chemical change. In particular, the organic acids induced a promotion of metal precipitation and thus an improvement in water quality that was attenuated in irradiated sediments. As these water chemistry changes are microbial driven it would be expected that the carbon addition would result in a marked change in the microbial community, and this is what was observed in the bacterial community profile, with a reduction in taxa diversity and a dominance of specific taxa. Previous studies have demonstrated that specific organic compounds enhance certain microbial organisms in AMD treatment systems, with different carbon substrates, acting as electron donors, selecting for different bacterial taxa (Salomo et al., 2009). For example, Jimenez-Castaneda et al. (2020) demonstrated that the addition of different complex (e.g. plant biomass) or simple (e.g. glycerol) carbon sources to acid rock drainage sediment microcosms resulted in markedly different microbial communities. While we examined responses to a mixed carbon solution containing ten different organic acids, in order to attempt to avoid selection of very specific bacterial taxa through use of a single organic acid, such as acetic acid, further studies could attempt to discriminate whether specific organic acids are of particular importance in determining this community profile. For example, Macias-Benitez et al. (2020) examined the consequence of lactic acid, oxalic acid or citric acid addition to biochemical function and bacterial community structure, finding that all three

489 organic acids decreased the diversity of a soil microbial community but that each organic
490 acid induced distinct responses.
491 The addition of organic acids resulted in decreased diversity, reduced evenness, and
492 increased dominance. This reflected an increased proportion of Desulfuromonadales, and in
493 particular *Geobacter* (Geobacteraceae) and *Pelobacter* (Pelobacteraceae). Both taxa have
494 previously been identified in AMD impacted natural environments (Hao et al., 2007;
495 Desoeuvre et al., 2016) and in passive and biological AMD treatments (Grubb et al., 2018;
496 Roth et al., 2019). Moreover, previous research has shown that *Geobacter* populations are
497 promoted by addition of acetic acid and lactic acid rather than other carbon sources such as
498 glucose, which can be utilised by a much wider range of bacteria (Ai et al., 2020). *Geobacter*
499 spp. including *Geobacter metallireducens* and *Geobacter sulfurreducens* can perform
500 dissimilatory Fe and other trace metal reduction via the utilisation of organic acids such as
501 acetic acid as an electron donor (Lovley et al., 1993; Caccavo et al., 1994; Mahadevan et al.,
502 2006). Therefore the dominance of specific taxa, including *Geobacter* following organic acid
503 amendment, is likely to increase metal cycling within the sediment as precipitated Fe and
504 other metals become deposited. *Geobacter* was first classified as a strict anaerobe
505 (Caccavo et al., 1994) but further studies have shown that *Geobacter* can tolerate oxygen in
506 sediments where physical disturbance facilitates its entry (Lin et al., 2004). In fact, increased
507 oxygen availability in the LOX sediments had no effect on *Geobacter* abundance as a similar
508 proportion was observed in both the LOA (without aeration) and LOX (with aeration)
509 microcosms. The genus *Pelobacter* consists of strictly anaerobic bacteria with a capacity to
510 utilise butyric acid and propionic acid as carbon sources (Krieg and Holt, 1984). *Pelobacter*
511 spp. have been found to have a phylogenetic relationship with known SRB and with
512 *Geobacter* spp. (Stackebrandt et al., 1989; Castro et al., 2000), which could explain why the
513 abundance of *Pelobacter* followed a similar pattern to that of *Geobacter*. Furthermore, there
514 is evidence that some *Pelobacter* spp. (e.g. *Pelobacter carbinolicus*) can perform Fe(III)
515 reduction like *Geobacter* and may also be capable of reducing elemental S (Lovley et al.,

1995). It has been shown that Fe(III) reduction can also lead to an increase in pH (Adams et al., 2007; Jimenez-Castaneda et al., 2020), and so is beneficial to AMD remediation.

Selection of different microbial community structures and thus different genomes will alter the functional potential of the sediment environment due to different profiles of functional genes and therefore a change in biogeochemical cycling. The change in the microbial community to a dominance by Geobacteraceae in response to organic acid addition is also reflected in the increased relative abundance of specific gene classes. For example, the increase in genes related to Fe acquisition and homeostasis in the LOA and LOX treatments is explained in part by the positive selection of *Geobacter* and the critical role of Fe in *Geobacter* metabolism, which generates several gene products related to Fe homeostasis (Embree et al., 2014). Furthermore, dissimilatory Fe(III) reduction is predominantly mediated by Geobacteraceae in many subsurface sediment environments (Holmes et al., 2002). While significant changes in Fe chemistry, including increased Fe^{3+} concentration, were observed in the LOA and LOX microcosms, the genetics underlying Fe oxidation and reduction reactions is poorly understood and not well annotated in gene annotation pipelines, including MG-RAST used here (Garber et al., 2020).

Our observations are indicative of the role of organic carbon amendments in promoting dissimilatory sulfate reduction activity. Previous work has demonstrated the role of organic acids such as acetic acid in modulating dissimilatory sulfate reduction activity in aquifers (Chapelle and Lovley, 1992) and organic acids have been used in reactors to enhance sulfate reduction (Liu et al., 2015). Likewise, dissimilatory sulfate reduction is important in AMD remediation processes in constructed wetlands by inducing alkalinity and enhancing metal precipitation (Mitsch and Wise, 1998). This enhanced sulfate reduction correlates with increased relative abundance of some specific S metabolism genes within the LOA and LOX metagenomes. These include a predicted adenylsulfate reductase (3.2- and 4.7-fold increased gene abundance in LOA and LOX, respectively) that plays a key role in sulfate to sulfide reduction in some sulfate-assimilating bacteria (Bick et al., 2000), and a dissimilatory sulfite reductase, which was particularly prevalent in the LOA metagenomes

(5.2-fold increased gene abundance relative to UNT). It is unclear which specific taxa might explain the increased sulfite reductase gene abundance. While DsrAB-type dissimilatory (bi)sulfite reductase enzymes encoded by *dsrAB* genes are present in many well-characterised SRB such as *Desulfovibrio* spp. (Karkhoff-Schweizer et al., 1995), there is no current evidence from the literature (Müller et al., 2015) and from publically available genomic data (including the metagenomics data from this study) that *Geobacter* spp. or *Pelobacter* spp. contain *dsrAB* genes, indicating that sulfate reduction activities are not directly due to these organisms. *Desulfovibrio* sp. and other potential SRB, including other Desulfovibrionaceae were only moderately enhanced in LOA and LOX samples compared to the OXY treatment, and were present with low abundance (*Desulfovibrio* sp. comprised 0.98% and 0.97% of the LOA and LOX taxa abundance, respectively). However, this and other low abundant taxa may still play important functional roles and could be responsible for the majority of the sulfate reduction activities taking place. For example, analysis of a peatland soil found that a *Desulfosporosinus* sp. with only 0.006% of the total taxa abundance accounted for most of the sulfate reduction activity (Pester et al., 2010).

Another marked change to the functional gene profiles in response to organic acid treatments was related to carbohydrate metabolism and respiration. The relative abundances of many genes related to carbohydrate metabolism were reduced in the LOA and LOX treatments in comparison to OXY and UNT. These included genes involved in the metabolism of sugars and degradation of compounds such as cellulose and other plant-derived polysaccharides, which are likely to be abundant within the organic-rich natural wetland sediment, but they are predicted to be metabolised at a reduced extent when there is high organic acid availability. In contrast, the relative abundances of genes related to respiration were significantly increased in both of the organic acid-rich LOA and LOX microcosms. Previous studies have shown that *Geobacter* respiration (as indicated by the expression of key respiratory genes including fumarate reductase and an outer membrane c-type cytochrome) is positively linked to availability of an electron donor such as acetic acid (Chin et al., 2004).

572 The OXY treatment showed an increase in oxidative stress genes and many S
573 metabolism genes, which coincides with an increase in *Sideroxydans* population. It is known
574 that *Sideroxydans* spp. can metabolise Fe coupled with oxygen reduction under aerobic
575 conditions (Beckwith et al., 2015). For this, many cytochrome-like proteins are used that can
576 also play a role in overall stress mitigation due to metal exposure (Chandrangsu et al.,
577 2017). Some thiosulfate and Fe sulfide oxidisers have been detected as related to the
578 *Sideroxydans* group which could explain the increase in S metabolism genes within the OXY
579 samples (Purcell et al., 2014).
580 With regard to the management of constructed wetlands or compost bioreactors for
581 AMD remediation, these results indicate the importance of maintaining a readily bioavailable
582 organic matter source but also indicate that while additional aeration may not provide further
583 substantial water quality benefits, the system does not need to be kept completely anoxic.
584 Future investigations might examine the role of different organic carbon sources, such as the
585 individual organic acids from the mixture used here, as well as more complex organic matter,
586 for driving specific biochemical reactions by particular bacterial strains to further optimise
587 water quality improvement of a semi-passive system. Although this study indicates that a
588 reduction in microbial diversity and dominance of specific taxa such as *Geobacter* might be
589 desirable in an AMD treatment system, other studies have demonstrated that such
590 community characteristics are not essential for successful remediation. For example,
591 previous examination of natural wetland sediments in the field indicates that AMD
592 bioremediation can still be achieved by maintaining high microbial diversity (Aguinaga et al.,
593 2018). The microcosms designed for this study were a simple artificial system and perhaps
594 the lack of wetland plants coupled with the addition of simple organic carbon inputs further
595 exacerbated the dominance of certain taxa and loss of diversity. Therefore additional
596 analyses of natural systems are still needed to better understand the processes taking place
597 within natural wetland sediments in order to better design the development of artificial AMD
598 remediation systems.
599

5. Conclusion

This study has demonstrated that the addition of organic carbon is more important in the development of an efficient semi-passive AMD treatment system than the availability of oxygen to the system, yet the presence of oxygen did not inhibit organic carbon-induced benefits. Changes in taxonomic composition of bacteria, predominantly in response to organic acid addition with or without aeration, suggested that a reduction in bacterial diversity and dominance of specific taxa, including members of *Geobacter* and *Pelobacter* spp., are likely to have enhanced specific metabolic activities including those associated with respiration, and Fe transformation and homeostasis. In contrast, there were no substantial alterations in archaeal and fungal community structures. These changes to sediment microbiology were coincident with enhanced trace metal precipitation and therefore an improvement in water quality, which are likely due to enhanced microbial sulfate reduction, but the exact microorganisms responsible for these activities were not determined. These insights should aid understanding of how to improve the efficiency of passive AMD treatments.

Acknowledgements

This work was supported by PhD scholarship funding (to OEA) from the National Fund for Scientific, Technological Development and Technological Innovation (FONDECYT) of Peru. We acknowledge the assistance of Paul Lythgoe for ICP-AES analysis and Debbie Ashworth for carbon measurements.

Authorship contribution statement

Oscar Aguinaga: Funding acquisition, Conceptualization, Methodology, Investigation, Data curation, Formal analysis, Writing – Original Draft, Visualization. **Keith White**: Conceptualization, Supervision, Project administration, Writing – Review & Editing. **Andrew Dean**: Conceptualization, Supervision, Writing – Review & Editing. **Jon Pittman**:

Conceptualization, Supervision, Project administration, Visualization, Writing – Review & Editing.

References

Adams, L.K., Harrison, J.M., Lloyd, J.R., Langley, S., Fortin, D., 2007. Activity and diversity of Fe(III)-reducing bacteria in a 3000-year-old acid mine drainage site analogue. Geomicrobiology Journal 24, 295-305.

Aguinaga, O.E., McMahon, A., White, K.N., Dean, A.P., Pittman, J.K., 2018. Microbial community shifts in response to acid mine drainage pollution within a natural wetland ecosystem. Frontiers in Microbiology 9, 1445.

Aguinaga, O.E., Wakelin, J.F.T., White, K.N., Dean, A.P., Pittman, J.K., 2019. The association of microbial activity with Fe, S and trace element distribution in sediment cores within a natural wetland polluted by acid mine drainage. Chemosphere 231, 432-441.

Ai, C., Yan, Z., Hou, S., Zheng, X., Zeng, Z., Amanze, C., Dai, Z., Chai, L., Qiu, G., Zeng, W., 2020. Effective treatment of acid mine drainage with microbial fuel cells: an emphasis on typical energy substrates. Minerals 10, 5.

August, E.E., McKnight, D.M., Hrncir, D.C., Garhart, K.S., 2002. Seasonal variability of metals transport through a wetland impacted by mine drainage in the Rocky Mountains. Environmental Science & Technology 36, 3779-3786.

Azapagic, A., 2004. Developing a framework for sustainable development indicators for the mining and minerals industry. Journal of Cleaner Production 12, 639-662.

Beckwith, C.R., Edwards, M.J., Lawes, M., Shi, L., Butt, J.N., Richardson, D.J., Clarke, T.A., 2015. Characterization of MtoD from *Sideroxydans lithotrophicus*: a cytochrome c electron shuttle used in lithoautotrophic growth. Frontiers in Microbiology 6, 332.

Bick, J.A., Dennis, J.J., Zylstra, G.J., Nowack, J., Leustek, T., 2000. Identification of a new class of 5′-adenylylsulfate (APS) reductases from sulfate-assimilating bacteria. Journal of Bacteriology 182, 135-142.

655 Bolger, A.M., Lohse, M., Usadel, B., 2014. Trimmomatic: a flexible trimmer for Illumina
656 sequence data. Bioinformatics 30, 2114-2120.
657 Caccavo, F., Lonergan, D.J., Lovley, D.R., Davis, M., Stolz, J.F., McInerney, M.J., 1994.
658 *Geobacter sulfurreducens* sp. nov., a hydrogen- and acetate-oxidizing dissimilatory
659 metal-reducing microorganism. Applied and Environmental Microbiology 60, 3752.
660 Canfield, D.E., Des Marais, D.J., 1991. Aerobic sulfate reduction in microbial mats. Science
661 251, 1471.
662 Castro, H.F., Williams, N.H., Ogram, A., 2000. Phylogeny of sulfate-reducing bacteria. FEMS
663 Microbiology Ecology 31, 1-9.
664 Chandrangsu, P., Rensing, C., Helmann, J.D., 2017. Metal homeostasis and resistance in
665 bacteria. Nature Reviews Microbiology 15, 338-350.
666 Chapelle, F.H., Lovley, D.R., 1992. Competitive exclusion of sulfate reduction by Fe(lll)-
667 reducing bacteria: a mechanism for producing discrete zones of high-iron ground
668 water. Groundwater 30, 29-36.
669 Chen, C.-J., Jiang, W.-T., 2012. Influence of waterfall aeration and seasonal temperature
670 variation on the iron and arsenic attenuation rates in an acid mine drainage system.
671 Applied Geochemistry 27, 1966-1978.
672 Chen, L.-x., Huang, L.-n., Méndez-García, C., Kuang, J.-l., Hua, Z.-s., Liu, J., Shu, W.-s.,
673 2016. Microbial communities, processes and functions in acid mine drainage
674 ecosystems. Current Opinion in Biotechnology 38, 150-158.
675 Chin, K.-J., Esteve-Núñez, A., Leang, C., Lovley, D.R., 2004. Direct correlation between
676 rates of anaerobic respiration and levels of mRNA for key respiratory genes in
677 *Geobacter sulfurreducens*. Applied and Environmental Microbiology 70, 5183-5189.
678 Clarke, K.R., 1993. Non-parametric multivariate analyses of changes in community structure.
679 Australian Journal of Ecology 18, 117-143.
680 Clyde, E.J., Champagne, P., Jamieson, H.E., Gorman, C., Sourial, J., 2016. The use of a
681 passive treatment system for the mitigation of acid mine drainage at the Williams

682 Brothers Mine (California): pilot-scale study. Journal of Cleaner Production 130, 116-
683 125.
684 Costa, M.C., Duarte, J.C., 2005. Bioremediation of acid mine drainage using acidic soil and
685 organic wastes for promoting sulphate-reducing bacteria activity on a column reactor.
686 Water, Air, and Soil Pollution 165, 325-345.
687 Das, B.K., Roy, A., Koschorreck, M., Mandal, S.M., Wendt-Potthoff, K., Bhattacharya, J.,
688 2009. Occurrence and role of algae and fungi in acid mine drainage environment with
689 special reference to metals and sulfate immobilization. Water Research 43, 883-894.
690 de Vet, W.W.J.M., Dinkla, I.J.T., Rietveld, L.C., van Loosdrecht, M.C.M., 2011. Biological
691 iron oxidation by *Gallionella* spp. in drinking water production under fully aerated
692 conditions. Water Research 45, 5389-5398.
693 Dean, A.P., Lynch, S., Rowland, P., Toft, B.D., Pittman, J.K., White, K.N., 2013. Natural
694 wetlands are efficient at providing long-term metal remediation of freshwater systems
695 polluted by acid mine drainage. Environmental Science & Technology 47, 12029-
696 12036.
697 Desoeuvre, A., Casiot, C., Héry, M., 2016. Diversity and distribution of arsenic-related genes
698 along a pollution gradient in a river affected by acid mine drainage. Microbial Ecology
699 71, 672-685.
700 Elliott, P., Ragusa, S., Catcheside, D., 1998. Growth of sulfate-reducing bacteria under
701 acidic conditions in an upflow anaerobic bioreactor as a treatment system for acid
702 mine drainage. Water Research 32, 3724-3730.
703 Embree, M., Qiu, Y., Shieu, W., Nagarajan, H., Neil, R., Lovley, D., Zengler, K., 2014. The
704 iron stimulon and Fur regulon of *Geobacter sulfurreducens* and their role in energy
705 metabolism. Applied and Environmental Microbiology 80, 2918.
706 Fernandez-Rojo, L., Héry, M., Le Pape, P., Braungardt, C., Desoeuvre, A., Torres, E., Tardy,
707 V., Resongles, E., Laroche, E., Delpoux, S., Joulian, C., Battaglia-Brunet, F.,
708 Boisson, J., Grapin, G., Morin, G., Casiot, C., 2017. Biological attenuation of arsenic

709 and iron in a continuous flow bioreactor treating acid mine drainage (AMD). Water
710 Research 123, 594-606.
711 Garber, A.I., Nealson, K.H., Okamoto, A., McAllister, S.M., Chan, C.S., Barco, R.A., Merino,
712 N., 2020. FeGenie: a comprehensive tool for the identification of iron genes and iron
713 gene neighborhoods in genome and metagenome assemblies. Frontiers in
714 Microbiology 11, 37.
715 Gibert, O., de Pablo, J., Luis Cortina, J., Ayora, C., 2004. Chemical characterisation of
716 natural organic substrates for biological mitigation of acid mine drainage. Water
717 Research 38, 4186-4196.
718 Grubb, D.G., Landers, D.G., Guerra, P.A., Miller, B., Bilgin, A., Hernandez, M.T., 2018.
719 Sugarcane bagasse as a microbial host media for the passive treatment of acid mine
720 drainage. Journal of Environmental Engineering 144, 04018108.
721 Hammer, Ø., Harper, D., Ryan, P., 2001. PAST-palaeontological statistics, ver. 1.89.
722 Palaeontologia Electronica 4, 1-9.
723 Hao, C., Zhang, H., Haas, R., Bai, Z., Zhang, B., 2007. A novel community of acidophiles in
724 an acid mine drainage sediment. World Journal of Microbiology and Biotechnology
725 23, 15-21.
726 Hedrich, S., Johnson, D.B., 2014. Remediation and selective recovery of metals from acidic
727 mine waters using novel modular bioreactors. Environmental Science & Technology
728 48, 12206-12212.
729 Hiibel, S.R., Pereyra, L.P., Breazeal, M.V.R., Reisman, D.J., Reardon, K.F., Pruden, A.,
730 2011. Effect of organic substrate on the microbial community structure in pilot-scale
731 sulfate-reducing biochemical reactors treating mine drainage. Environmental
732 Engineering Science 28, 563-572.
733 Holmes, D.E., Finneran, K.T., O'Neil, R.A., Lovley, D.R., 2002. Enrichment of members of
734 the family *Geobacteraceae* associated with stimulation of dissimilatory metal
735 reduction in uranium-contaminated aquifer sediments. Applied and Environmental
736 Microbiology 68, 2300-2306.

737 Huang, L.-N., Kuang, J.-L., Shu, W.-S., 2016. Microbial ecology and evolution in the acid
738 mine drainage model system. Trends in Microbiology 24, 581-593.
739 Huang, Y., Ortiz, L., Aguirre, P., García, J., Mujeriego, R., Bayona, J.M., 2005. Effect of
740 design parameters in horizontal flow constructed wetland on the behaviour of volatile
741 fatty acids and volatile alkylsulfides. Chemosphere 59, 769-777.
742 Jayalath, N., Fitzpatrick, R.W., Mosley, L., Marschner, P., 2016. Type of organic carbon
743 amendment influences pH changes in acid sulfate soils in flooded and dry conditions.
744 Journal of Soils and Sediments 16, 518-526.
745 Jimenez-Castaneda, M.E., Scarinci, C., Burke, A., Boothman, C., Vaughan, D.J., Lloyd, J.R.,
746 van Dongen, B.E., 2020. Generation of alkalinity by stimulation of microbial iron
747 reduction in acid rock drainage systems: impact of natural organic matter types.
748 Water, Air, & Soil Pollution 231, 472.
749 Johnson, D.B., Hallberg, K.B., 2005. Acid mine drainage remediation options: a review.
750 Science of the Total Environment 338, 3-14.
751 Johnson, D.B., Kanao, T., Hedrich, S., 2012. Redox transformations of iron at extremely low
752 pH: fundamental and applied aspects. Frontiers in Microbiology 3, 96.
753 Karimian, N., Johnston, S.G., Burton, E.D., 2018. Iron and sulfur cycling in acid sulfate soil
754 wetlands under dynamic redox conditions: A review. Chemosphere 197, 803-816.
755 Karkhoff-Schweizer, R.R., Huber, D.P., Voordouw, G., 1995. Conservation of the genes for
756 dissimilatory sulfite reductase from *Desulfovibrio vulgaris* and *Archaeoglobus fulgidus*
757 allows their detection by PCR. Applied and Environmental Microbiology 61, 290-296.
758 Kirby, C.S., Dennis, A., Kahler, A., 2009. Aeration to degas CO_2, increase pH, and increase
759 iron oxidation rates for efficient treatment of net alkaline mine drainage. Applied
760 Geochemistry 24, 1175-1184.
761 Kjeldsen, K.U., Joulian, C., Ingvorsen, K., 2004. Oxygen tolerance of sulfate-reducing
762 bacteria in activated sludge. Environmental Science & Technology 38, 2038-2043.
763 Krieg, N.R., Holt, J.G., 1984. Bergey's Manual of Systematic Bacteriology. Williams and
764 Wilkins, Baltimore.

765 Lin, W.C., Coppi, M.V., Lovley, D.R., 2004. *Geobacter sulfurreducens* can grow with oxygen
766 as a terminal electron acceptor. Applied and Environmental Microbiology 70, 2525.
767 Liu, H., Hu, Z., Zhang, J., Ngo, H.H., Guo, W., Liang, S., Fan, J., Lu, S., Wu, H., 2016.
768 Optimizations on supply and distribution of dissolved oxygen in constructed wetlands:
769 A review. Bioresource Technology 214, 797-805.
770 Liu, Y., Zhang, Y., Ni, B.-J., 2015. Evaluating enhanced sulfate reduction and optimized
771 volatile fatty acids (VFA) composition in anaerobic reactor by Fe (III) addition.
772 Environmental Science & Technology 49, 2123-2131.
773 Lovley, D.R., Giovannoni, S.J., White, D.C., Champine, J.E., Phillips, E.J.P., Gorby, Y.A.,
774 Goodwin, S., 1993. *Geobacter metallireducens* gen. nov. sp. nov., a microorganism
775 capable of coupling the complete oxidation of organic compounds to the reduction of
776 iron and other metals. Archives of Microbiology 159, 336-344.
777 Lovley, D.R., Phillips, E.J., Lonergan, D.J., Widman, P.K., 1995. Fe(III) and S^0 reduction by
778 *Pelobacter carbinolicus*. Applied and Environmental Microbiology 61, 2132-2138.
779 Macias-Benitez, S., Garcia-Martinez, A.M., Caballero Jimenez, P., Gonzalez, J.M., Tejada
780 Moral, M., Parrado Rubio, J., 2020. Rhizospheric organic acids as biostimulants:
781 monitoring feedbacks on soil microorganisms and biochemical properties. Frontiers
782 in Plant Science 11, 633.
783 Mahadevan, R., Bond, D.R., Butler, J.E., Esteve-Nuñez, A., Coppi, M.V., Palsson, B.O.,
784 Schilling, C.H., Lovley, D.R., 2006. Characterization of metabolism in the Fe(III)-
785 reducing organism *Geobacter sulfurreducens* by constraint-based modeling. Applied
786 and Environmental Microbiology 72, 1558-1568.
787 Marschall, C., Frenzel, P., Cypionka, H., 1993. Influence of oxygen on sulfate reduction and
788 growth of sulfate-reducing bacteria. Archives of Microbiology 159, 168-173.
789 McNamara, N.P., Black, H.I.J., Beresford, N.A., Parekh, N.R., 2003. Effects of acute gamma
790 irradiation on chemical, physical and biological properties of soils. Applied Soil
791 Ecology 24, 117-132.

792 Meier, J., Piva, A., Fortin, D., 2012. Enrichment of sulfate-reducing bacteria and resulting
793 mineral formation in media mimicking pore water metal ion concentrations and pH
794 conditions of acidic pit lakes. FEMS Microbiology Ecology 79, 69-84.
795 Méndez-García, C., Peláez, A.I., Mesa, V., Sánchez, J., Golyshina, O.V., Ferrer, M., 2015.
796 Microbial diversity and metabolic networks in acid mine drainage habitats. Frontiers
797 in Microbiology 6, 475.
798 Meyer, F., Paarmann, D., D'Souza, M., Olson, R., Glass, E.M., Kubal, M., Paczian, T.,
799 Rodriguez, A., Stevens, R., Wilke, A., Wilkening, J., Edwards, R.A., 2008. The
800 metagenomics RAST server – a public resource for the automatic phylogenetic and
801 functional analysis of metagenomes. BMC Bioinformatics 9, 386.
802 Mitsch, W.J., Wise, K.M., 1998. Water quality, fate of metals, and predictive model validation
803 of a constructed wetland treating acid mine drainage. Water Research 32, 1888-
804 1900.
805 Moche, M., Gutknecht, J., Schulz, E., Langer, U., Rinklebe, J., 2015. Monthly dynamics of
806 microbial community structure and their controlling factors in three floodplain soils.
807 Soil Biology and Biochemistry 90, 169-178.
808 Mosier, A.C., Miller, C.S., Frischkorn, K.R., Ohm, R.A., Li, Z., LaButti, K., Lapidus, A.,
809 Lipzen, A., Chen, C., Johnson, J., Lindquist, E.A., Pan, C., Hettich, R.L., Grigoriev,
810 I.V., Singer, S.W., Banfield, J.F., 2016. Fungi contribute critical but spatially varying
811 roles in nitrogen and carbon cycling in acid mine drainage. Frontiers in Microbiology
812 7, 238.
813 Müller, A.L., Kjeldsen, K.U., Rattei, T., Pester, M., Loy, A., 2015. Phylogenetic and
814 environmental diversity of DsrAB-type dissimilatory (bi)sulfite reductases. The ISME
815 Journal 9, 1152-1165.
816 Neculita, C.-M., Zagury, G.J., Bussière, B., 2007. Passive treatment of acid mine drainage in
817 bioreactors using sulfate-reducing bacteria. Journal of Environmental Quality 36, 1-
818 16.

819 Overbeek, R., Olson, R., Pusch, G.D., Olsen, G.J., Davis, J.J., Disz, T., Edwards, R.A.,
820 Gerdes, S., Parrello, B., Shukla, M., Vonstein, V., Wattam, A.R., Xia, F., Stevens, R.,
821 2014. The SEED and the Rapid Annotation of microbial genomes using Subsystems
822 Technology (RAST). Nucleic Acids Research 42, D206-D214.
823 Pester, M., Bittner, N., Deevong, P., Wagner, M., Loy, A., 2010. A 'rare biosphere'
824 microorganism contributes to sulfate reduction in a peatland. The ISME Journal 4,
825 1591-1602.
826 Pruitt, K.D., Tatusova, T., Maglott, D.R., 2007. NCBI reference sequences (RefSeq): a
827 curated non-redundant sequence database of genomes, transcripts and proteins.
828 Nucleic Acids Research 35, D61-D65.
829 Purcell, A.M., Mikucki, J.A., Achberger, A.M., Alekhina, I.A., Barbante, C., Christner, B.C.,
830 Ghosh, D., Michaud, A.B., Mitchell, A.C., Priscu, J.C., Scherer, R., Skidmore, M.L.,
831 Vick-Majors, T.J., the WISSARD Science Team, 2014. Microbial sulfur
832 transformations in sediments from subglacial Lake Whillans. Frontiers in Microbiology
833 5, 594.
834 Roth, H., Gallo, S., Badger, P., Hillwig, M., 2019. Changes in microbial communities of a
835 passive coal mine drainage bioremediation system. Canadian Journal of
836 Microbiology 65, 775-782.
837 Salomo, S., Münch, C., Röske, I., 2009. Evaluation of the metabolic diversity of microbial
838 communities in four different filter layers of a constructed wetland with vertical flow by
839 Biolog™ analysis. Water Research 43, 4569-4578.
840 Seena, S., Sobral, O., Cano, A., 2020. Metabolomic, functional, and ecologic responses of
841 the common freshwater fungus *Neonectria lugdunensis* to mine drainage stress.
842 Science of the Total Environment 718, 137359.
843 Senko, J.M., Bertel, D., Quick, T.J., Burgos, W.D., 2011. The influence of phototrophic
844 biomass on Fe and S redox cycling in an acid mine drainage-impacted system. Mine
845 Water and the Environment 30, 38-46.

Stackebrandt, E., Wehmeyer, U., Schink, B., 1989. The phylogenetic status of *Pelobacter acidigallici*, *Pelobacter venetianus*, and *Pelobacter carbinolicus*. Systematic and Applied Microbiology 11, 257-260.

van der Graaf, C.M., Sánchez-España, J., Yusta, I., Ilin, A., Shetty, S.A., Bale, N.J., Villanueva, L., Stams, A.J.M., Sánchez-Andrea, I., 2020. Biosulfidogenesis mediates natural attenuation in acidic mine pit lakes. Microorganisms 8, 1275.

Wang, H., Zeng, Y., Guo, C., Bao, Y., Lu, G., Reinfelder, J.R., Dang, Z., 2018. Bacterial, archaeal, and fungal community responses to acid mine drainage-laden pollution in a rice paddy soil ecosystem. Science of the Total Environment 616-617, 107-116.

Webb, J.S., McGinness, S., Lappin-Scott, H.M., 1998. Metal removal by sulphate-reducing bacteria from natural and constructed wetlands. Journal of Applied Microbiology 84, 240-248.

Ye, F., Gong, D., Pang, C., Luo, J., Zeng, X., Shang, C., 2020. Analysis of fungal composition in mine-contaminated soils in Hechi City. Current Microbiology 77, 2685-2693.

Zhang, J., Kobert, K., Flouri, T., Stamatakis, A., 2014. PEAR: a fast and accurate Illumina Paired-End reAd mergeR. Bioinformatics 30, 614-620.

Zhang, M., Wang, H., 2014. Organic wastes as carbon sources to promote sulfate reducing bacterial activity for biological remediation of acid mine drainage. Minerals Engineering 69, 81-90.

Figures

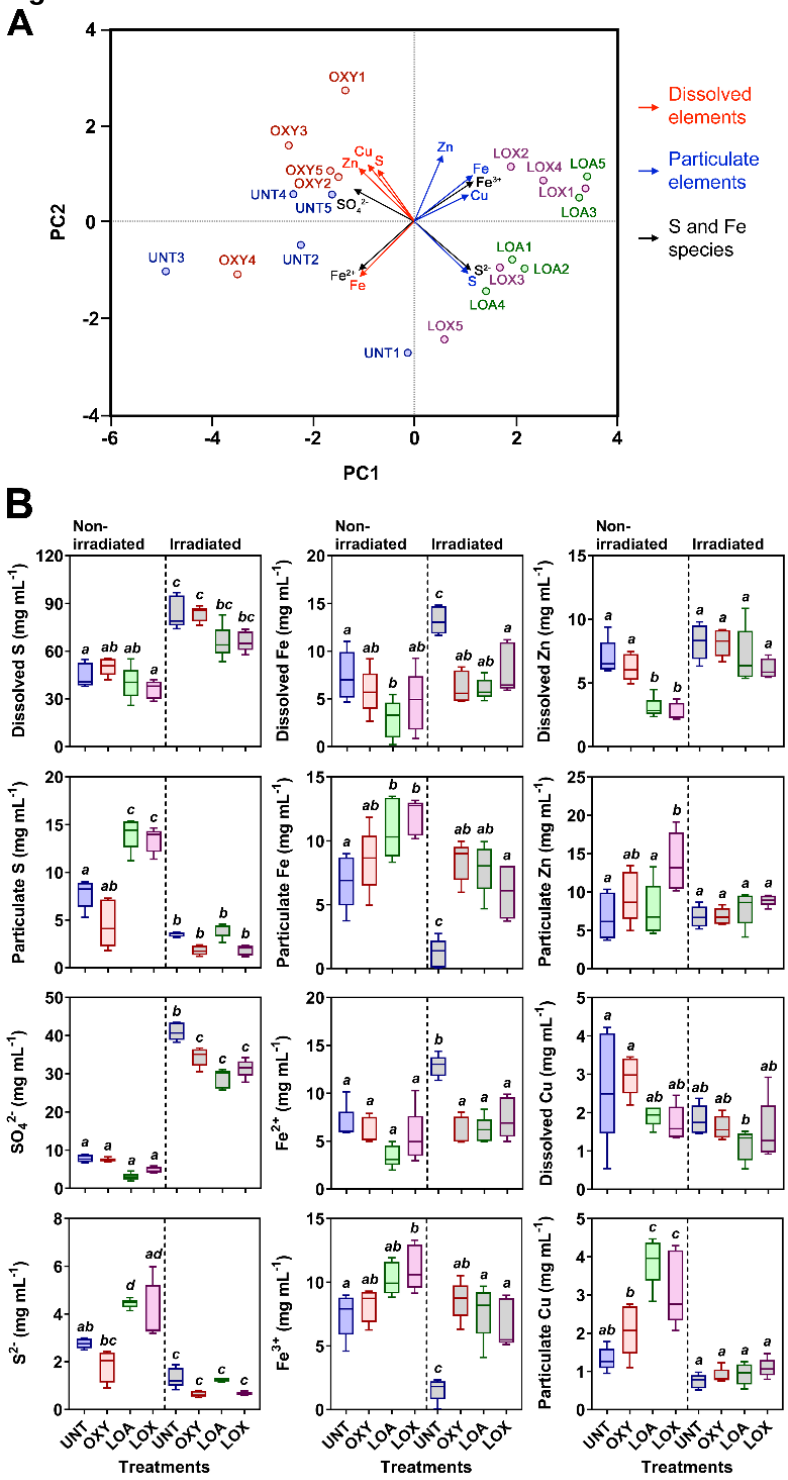

Fig. 1. Water chemistry characteristics in microcosms at the end of the incubation period. (A) PCA comparing water chemistry characteristics from non-irradiated microcosms for each treatment. PC1 and PC2 contribute 52.1% and 16.4% variance of the data, respectively. Dissolved Cu, Fe, S and Zn are indicated by red loading vectors, particulate Cu, Fe, S and Zn are indicated by blue loading vectors, and Fe^{2+}, Fe^{3+}, SO_4^{2-} and S^{2-} are indicated by black loading vectors. (B) Concentrations of indicated chemicals in the water of each microcosm at the end of the incubation period for non-irradiated and gamma irradiated sediment microcosms. Data are from five replicate microcosms for each treatment. Boxes show the 25th and 75th percentiles, the line within the boxes shows the median values. Whisker bars show the minimum and maximum values. Boxes that do not share lowercase letters are significantly different ($p < 0.05$). UNT: untreated, OXY: oxygenated by aeration, LOA: low molecular weight organic acids, LOX: organic acids and aeration.

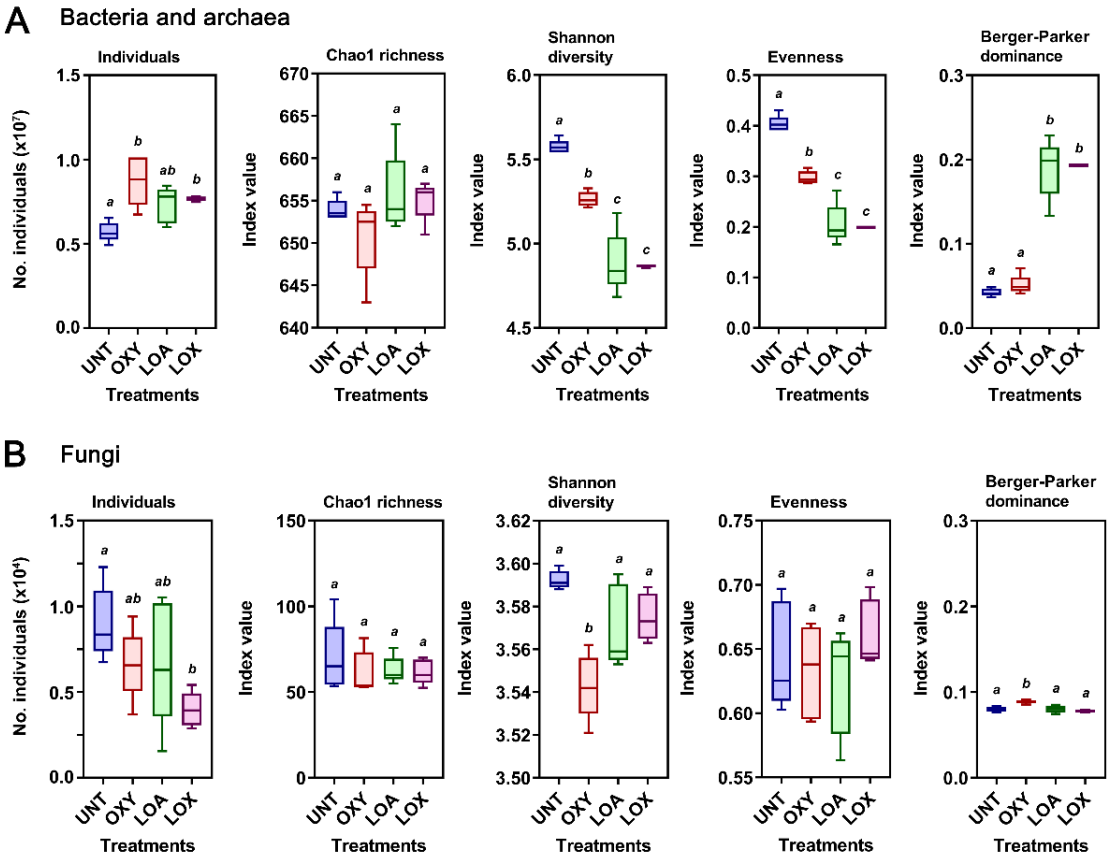

Fig. 2. Bacteria and archaea (A) and fungi (B) community diversity values determined from genus level data from the sediment for each treatment at the end of the incubation period. Data are from five replicate microcosms for each treatment. UNT: untreated, OXY: oxygenated by aeration, LOA: low molecular weight organic acids, LOX: organic acids and aeration. Boxes show the 25th and 75th percentiles, the line within the boxes shows the median values. Whisker bars show the minimum and maximum values. Boxes that do not share lowercase letters are significantly different ($p < 0.05$).

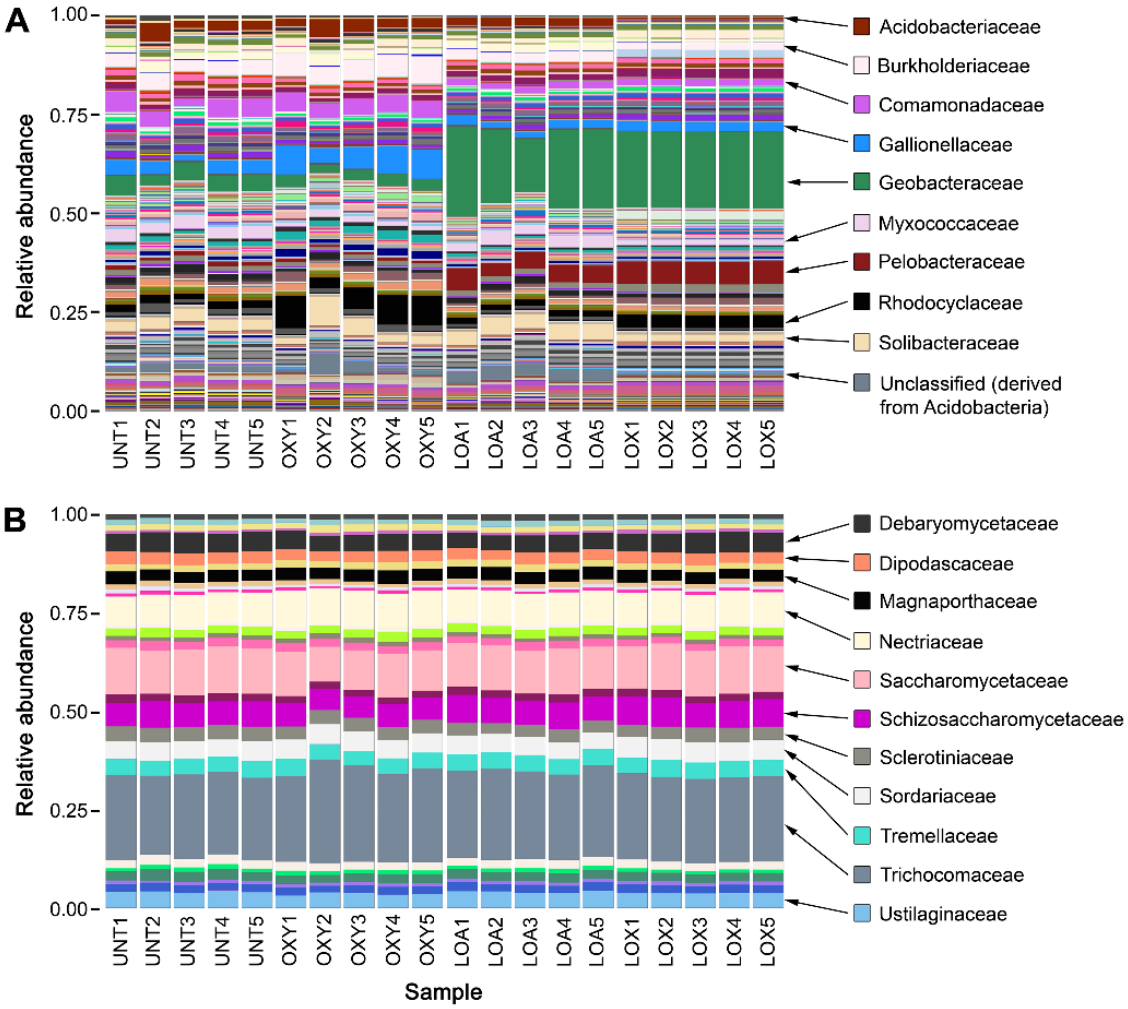

Fig. 3. Relative abundance of bacteria and archaea (A) and fungi (B) at family level within the sediment for each treatment at the end of the incubation period. Data are from five replicate microcosms for each treatment. UNT: untreated, OXY: oxygenated by aeration, LOA: low molecular weight organic acids, LOX: organic acids and aeration. Selected taxa with highest abundance in multiple samples are labelled.

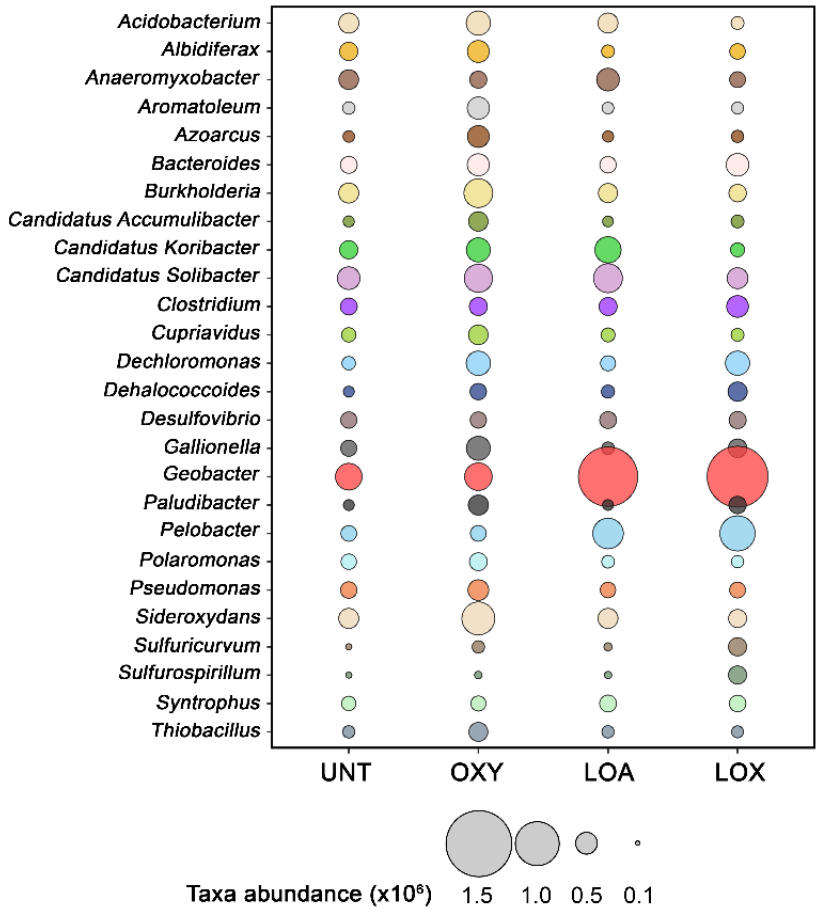

Fig. 4. Representation of mean abundance values of individual bacterial taxa at genus level that were identified by SIMPER analysis to give the most contribution to each treatment community assemblage. Data are from the five replicate microcosms for each treatment at the end of the incubation period. UNT: untreated, OXY: oxygenated by aeration, LOA: low molecular weight organic acids, LOX: organic acids and aeration.

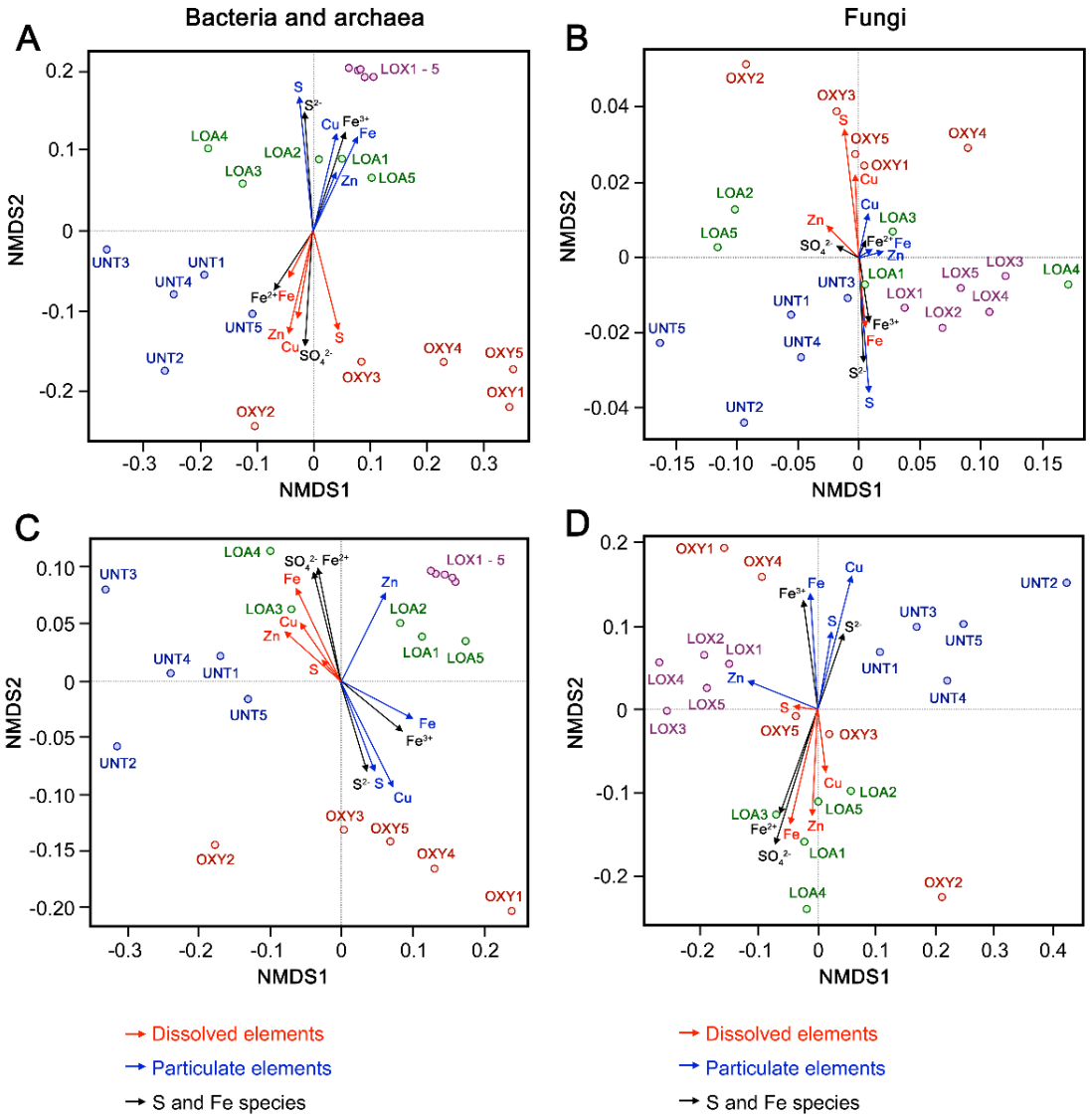

Fig. 5. Discrimination of the replicate microcosms for each treatment at the end of the incubation period on the basis of taxonomic similarities at family level (A and B) between bacteria and archaea (A) and fungi (B), and on the basis of functional gene (metagenome) similarities (C and D) between bacteria and archaea (C) and fungi (D). Dissolved Cu, Fe, S and Zn are indicated by red loading vectors, particulate Cu, Fe, S and Zn are indicated by blue loading vectors, and Fe^{2+}, Fe^{3+}, SO_4^{2-} and S^{2-} are indicated by black loading vectors. UNT: untreated, OXY: oxygenated by aeration, LOA: low molecular weight organic acids, LOX: organic acids and aeration.

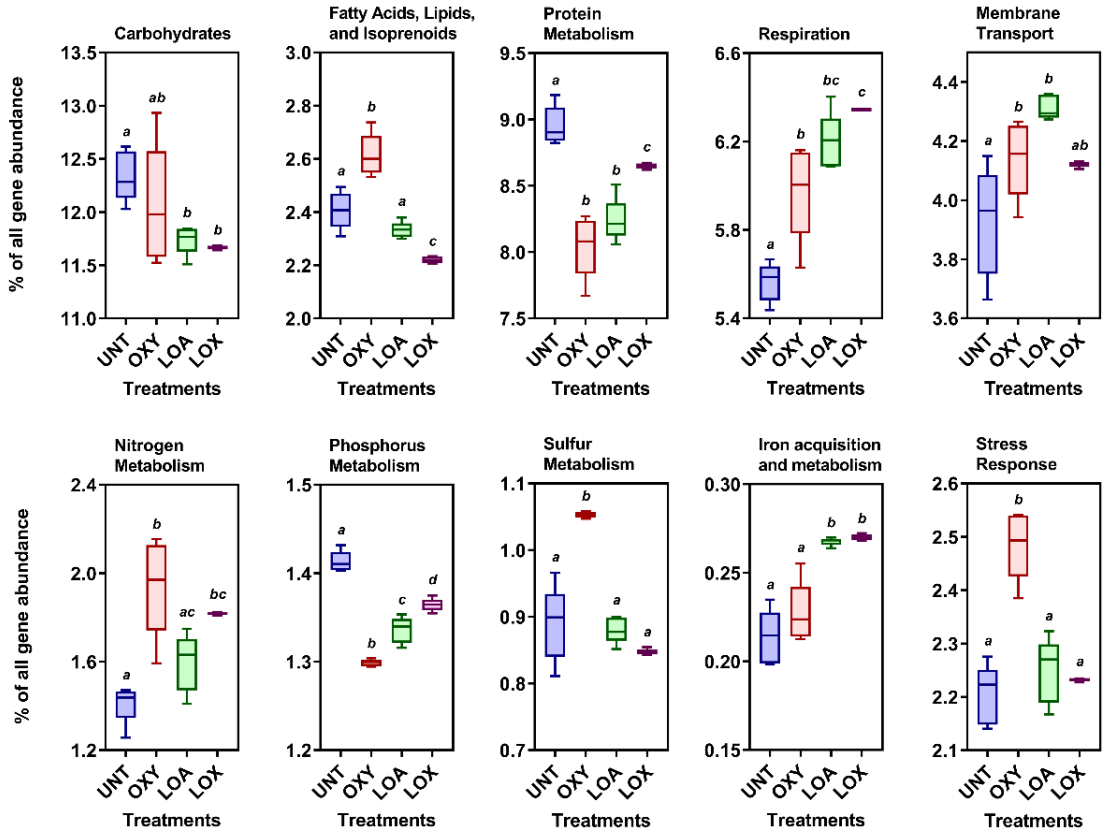

Fig. 6. Relative gene abundance values of selected functional classes related to metabolism, membrane transport and stress response determined from bacteria and archaea metagenome data at the end of the incubation period. Data are from five replicate microcosms for each treatment. UNT: untreated, OXY: oxygenated by aeration, LOA: low molecular weight organic acids, LOX: organic acids and aeration. Boxes show the 25th and 75th percentiles, the line within the boxes shows the median values. Whisker bars show the minimum and maximum values. Boxes that do not share lowercase letters are significantly different ($p < 0.05$).